Supplement of Atmos. Chem. Phys., 16, 7917–7941, 2016
http://www.atmos-chem-phys.net/16/7917/2016/
doi:10.5194/acp-16-7917-2016-supplement

Atmospheric Chemistry and Physics Open Access EGU

Supplement of

Rethinking the global secondary organic aerosol (SOA) budget: stronger production, faster removal, shorter lifetime

Alma Hodzic et al.

Correspondence to: Alma Hodzic (alma@ucar.edu)

Sect. S1: Isoprene-specific SOM scheme

The statistical oxidation model [*Cappa and Wilson*, 2012] was developed to simulate the multi-generational reactions associated with oxidation (functionalization and fragmentation) of volatile organic compounds (VOCs) within a medium-complexity framework (when compared to models that don't treat ageing explicitly, such as the 2-product model, or to fully-explicit models, such as GECKO-A or MCM). The original [*Cappa and Wilson,* 2012] and updated [*Zhang et al.,* 2014] SOM framework assumes that the reactivity of all "product" species can be described based only on the number of carbon (n_C) and oxygen (n_O) atoms making up that SOM species. The dependence of the SOM rate coefficients on n_C and n_O was determined based on an assessment of the output from the GECKO-A model for multi-component simulations run based on mixture of organic compounds that is representative of Mexico City [*Zhang et al.,* 2014]. For species containing multiple double bonds, such as isoprene, the original SOM framework may not properly reflect the enhanced reactivity of some of the early-generation product species due to the presence of a residual double bond. Here, we focus on isoprene.

The products formed from isoprene photooxidation depend importantly on whether the intermediate peroxy radicals react with NO or with HO_2 or RO_2 or whether the molecule isomerizes. Generally speaking, one can distinguish between "low-NO_x" conditions (where reactions with HO_2 dominate) or "high-NO_x" conditions (where reactions with NO dominate). Considering first low-NO_x conditions, as an example, one key product from oxidation of isoprene by OH radicals conditions is the double-bond containing isoprene hydroxy hydroperoxide (ISOPOOH, $C_5H_{10}O_3$) [*Surratt et al.,* 2010]. ISOPOOH reacts rapidly with OH radicals, with room-temperature rate coefficients of k_{OH} = 7.5 x 10^{-11} cm^3 $molecule^{-1}$ s^{-1} for the (1,2)- isomer and k_{OH} = 11.8 x 10^{-11} cm^3 $molecule^{-1}$ s^{-1} for the (4,3)-isomer [*St. Clair et al.,* 2015]. These are comparable with the isoprene rate coefficient for reaction with OH, which is k_{OH} = 10 x 10^{-11} cm^3 $molecule^{-1}$ s^{-1}, but much larger than the original SOM k_{OH} for the C_5O_3 species ($k_{OH,SOM}$ = 0.72 x 10^{-11} cm^3 $molecule^{-1}$ s^{-1}). Other key product species formed from multi-generational isoprene photooxidation, such as isoprene epoxydiols (IEPOX), react with rate coefficients more similar to those used with the original SOM. For example, estimates of the k_{OH} for IEPOX range from 0.84 x 10^{-11} to 3.5 x 10^{-11} cm^3 $molecule^{-1}$ s^{-1} [*Jacobs et al.,* 2013; *Bates et al.,* 2014], which can be

compared with the SOM prediction for C_5O_3 ($k_{OH,SOM}$ = 0.72 x 10^{-11} cm^3 $molecule^{-1}$ s^{-1}). Altogether, this suggests that for VOC precursors such as isoprene the original SOM can substantially underestimate the reactivity of some of the early-generation product species in particular, when low-NO_x conditions prevail. Turning to high-NO_x conditions, key first-generation product species are methacrolein (MVK, C_4O_1) and methyl vinyl ketone (MVK, C_4O_1). Both of these react with OH with rate coefficients around 2-3 x 10^{-11} cm^3 $molecule^{-1}$ s^{-1} [*Paulot et al.,* 2009], which can be compared to the SOM rate coefficient for C_4O_1 of 0.96 x 10^{-11} cm^3 $molecule^{-1}$ s^{-1}. This suggests that although the SOM rate coefficient may be too low for these species, the discrepancy is not nearly as large as is possible for low-NO_x conditions, and further these key first generation products react much more slowly with OH than does isoprene.

Although the above discussion demonstrates that the chemistry governing isoprene oxidation is highly complex, it seems nonetheless useful to consider as an alternative method an isoprene-specific SOM scheme that attempts to account for this enhanced reactivity of some product species compared to the original SOM. The development of such a scheme in the SOM framework is complicated by isoprene product compounds (such as ISOPOOH and IEPOX) having the same n_C and n_O but very different rate coefficients for reaction with OH (and in SOM, all species with the same n_C and n_O are assumed to behave identically). Nevertheless, as a first effort towards an isoprene-specific SOM mechanism, an alternate SOM has been developed in which the original SOM k_{OH} relationship with (n_C,n_O) has been modified for the subset of species with n_C = 5 and $1 \leq n_O \leq 4$. Specifically, it is assumed that k_{OH} for all of these species (C_5O_1, C_5O_2, C_5O_3 and C_5O_4) are all the same as isoprene (C_5O_0), namely k_{OH} = 10 x 10^{-11} cm^3 $molecule^{-1}$ s^{-1}. Although certainly not a perfect representation of the complexity of isoprene oxidation, this modification nonetheless allows for faster reaction of a subset of products that correspond reasonably to "first generation." This alternate SOM formulation is likely to be most applicable to reactions occurring under low-NO_x conditions, since this is when the largest product k_{OH} values are obtained. The alternate SOM model has been fit to laboratory chamber data on isoprene SOA formation for experiments conducted under either low-NO_x or high-NO_x conditions [*Chhabra et al.,* 2011; *Zhang et al.,* 2014] to determine an alternative set of SOM parameters. The fits were conducted assuming that vapor wall losses influenced the experiment with a first-order loss coefficient of k_{wall} = 1 x 10^{-4} s^{-1} (as was done for all other species, discussed in

the main text). The resulting fits using alternate SOM are shown in Figure S1, along with the fits that resulted from the original SOM.

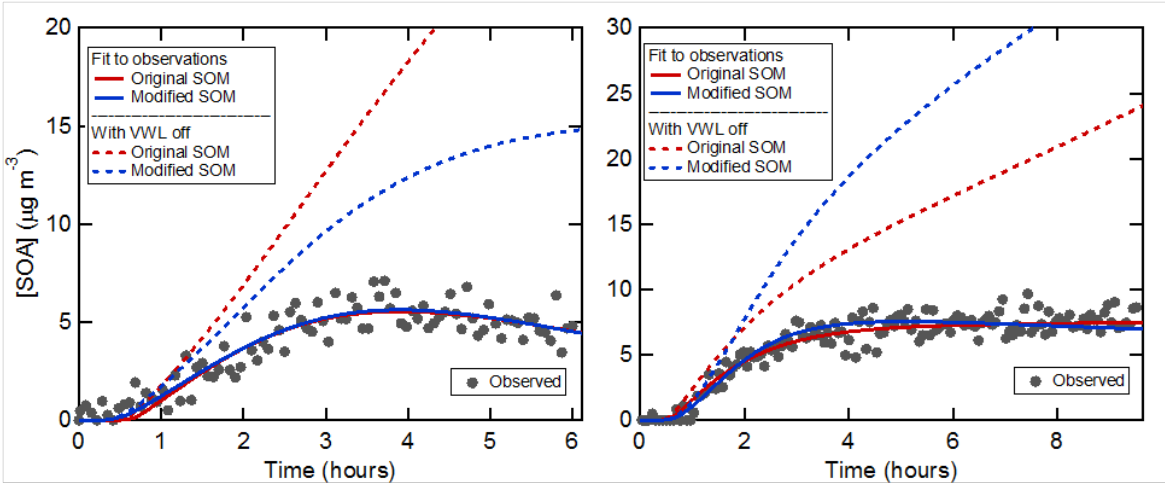

Figure S1. Observations of SOA formation (gray points) and the resulting SOM fits to the observations (solid lines) for the original SOM (red) and the modified SOM (blue), and where the fits were performed under the assumption that k_{wall} = 1 x 10^{-4} s^{-1}. SOM simulation results based on these fits are also shown for the same reaction conditions (i.e. initial VOC concentration, OH concentration), but where k_{wall} is now set to zero (dashed lines) to illustrate the influence that vapor wall losses had on the model fits. Observations and results are shown for low NO_x (left panel) and high NO_x (right panel) conditions, with more experimental details available in *Zhang et al.* [2014] and *Chhabra et al.* [2011].

The SOM parameters for this alternate fit are shown in Tables S1 and S2 along with the original SOM fits. It is evident that both model formulations (original or alternate SOM) fit the observations well. Using the fit parameters determined from this fitting exercise, simulations were then run where all conditions were the same as the experimental

conditions but now where the vapor wall loss rate coefficient was set to zero. This is meant to reflect what might happen in the atmosphere when the loss rate of vapors is decreased substantially relative to that in the chamber. For both the original and alternate SOM formulations, the amount of SOA simulated when k_{wall} = 0 is substantially increased relative to when k_{wall} = 1 x 10^{-4} s^{-1}, indicating the importance of accounting for vapor wall losses when fitting chamber observations. There are, however, notable differences between the two formulations that depend on the NO_x condition. For the low-NO_x case, the alternate formulation leads to less SOA than does the original formulation. For the high-NO_x case, the alternate formulation leads to more SOA than does the original formulation.

Additional simulations were run (similar to those in the main text for other species) to determine the long-time VBS product yields that describe the SOA formation from isoprene oxidation. Specifically, simulations were run for 36 h where [isoprene] = 1 ppt, [seed] = 10 $\mu g\ m^{-3}$, [OH] = 2 x 10^6 $molecule^{-1}\ cm^{-3}$, and where the seed is assumed to be absorbing and instantaneous equilibrium partitioning was assumed. At the end of these 36 h, the SOM products in both the gas and particle phases were binned according to saturation concentration (in $\mu g\ m^{-3}$) into logarithmically spaced bins ranging from log C^* of -2 to 3. All species with log C^* < -2 were grouped into the log C^* = -2 bin. The product mass yields for products in each bin were calculated by dividing the total mass concentration of all species in that bin by the amount of reacted isoprene. The SOA mass yield (calculated as new SOA formed divided by isoprene reacted) differed substantially between the simulations using the original and alternate formulations. For both low- and high-NO_x the SOA mass yield was much larger for the original formulation. For the low-NO_x case, this is primarily due to the difference in the predicted yield of species that fall into the log C^* = 1 bin. For the high-NO_x case the difference was primarily due to the larger yield of species in both the log C^* = 0 and 1 bins. This result indicates that structural assumptions regarding the SOM model can have a large impact on the simulated VBS mass yields and total SOA yield predicted by SOM.

Table S1. The derived SOM parameters for isoprene under low-NO_x and high-NO_x conditions derived from the original SOM formulation and for the alternate case in which some of the products are assumed to be more reactive towards OH radicals. The SOM fits used here were derived assuming that vapor wall losses influenced the observations, with k_{wall} = 1 x 10^{-4} s^{-1}.

SOM Parameter[a]	Low-NO_x		High-NO_x	
	Original	Alternate	Original	Alternate
m_{frag}	0.01	0.01	0.322	0.502
DLVP	2.23	2.25	2.23	1.92
P1	0.0003	0.789	0.679	0.994
P2	0.146	8E-05	0.321	4E-05
P3	0.826	0.183	0.0005	0.006
P4	0.028	0.028	0.0002	0.0002

See *Cappa and Wilson* [2012] for detailed descriptions of these parameters. In brief, m_{frag} characterizes the fragmentation probability with P_{frag} = $(O:C)^{mfrag}$, ΔLVP characterizes the decrease in volatility per oxygen atom added and P1-P4 indicate the probability of functionalization leading to addition of 1-4 oxygen atoms.

Table S2. Derived VBS mass yields for isoprene under low-NO_x and high-NO_x conditions derived from the original SOM formulation and for the alternate case in which some of the products are assumed to be more reactive towards OH radicals. The SOM fits used here were derived assuming that vapor wall losses influenced the observations, with k_{wall} = 1 x 10^{-4} s^{-1}.

	Low-NO_x		High-NO_x	
log C^*	Original	Alternate	Original	Alternate
-2	0.011	0.012	0.013	0.001
-1	0.014	0.013	0.008	0.000
0	0.042	0.001	0.079	0.027
1	0.333	0.100	0.083	0.021
2	0.216	0.078	0.059	0.044
3	0.348	0.097	0.178	0.185
SOA yield with 10 μg m^{-3} seed	**0.252**	**0.083**	**0.141**	**0.042**

Table S3. Derived VBS mass yields for isoprene under low-NO_x and high-NO_x conditions derived from the original SOM formulation and for the alternate case in which some of the products are assumed to be more reactive towards OH radicals. The SOM fits used here were derived assuming that vapor wall losses did not influence the observations, with k_{wall} = 0 s^{-1}.

	Low-NO_x		High-NO_x	
log C^*	Original	Alternate	Original	Alternate
-2	0.002	0.002	0.000	0.000
-1	0.001	0.027	0.000	0.002
0	0.044	0.000	0.008	0.000
1	0.010	0.019	0.007	0.021
2	0.000	0.023	0.025	0.026
3	0.054	0.003	0.018	0.007
SOA yield with 10 mg m^{-3} seed	**0.049**	**0.041**	**0.013**	**0.015**

Bates, K. H., Crounse, J. D., St. Clair, J. M., Bennett, N. B., Nguyen, T. B., Seinfeld, J. H., Stoltz, B. M., and Wennberg, P. O.: Gas Phase Production and Loss of Isoprene Epoxydiols, J. Phys. Chem. A, 118, 1237-1246, doi:10.1021/jp4107958, 2014.

Cappa, C. D. and Wilson, K. R.: Multi-generation gas-phase oxidation, equilibrium partitioning, and the formation and evolution of secondary organic aerosol, Atmos. Chem. Phys., 12, 9505-9528, doi:10.5194/acp-12-9505-2012, 2012.

Chhabra, P. S., Ng, N. L., Canagaratna, M. R., Corrigan, A. L., Russell, L. M., Worsnop, D. R., Flagan, R. C., and Seinfeld, J. H.: Elemental composition and oxidation of chamber organic aerosol, Atmos. Chem. Phys., 11, 8827-8845, doi:10.5194/acp-11-8827-2011, 2011.

Jacobs, M. I., Darer, A. I., and Elrod, M. J.: Rate Constants and Products of the OH Reaction with Isoprene-Derived Epoxides, Environ. Sci. Technol., 47, 12868-12876, doi:10.1021/es403340g, 2013.

Paulot, F., Crounse, J. D., Kjaergaard, H. G., Kroll, J. H., Seinfeld, J. H., and Wennberg, P. O.: Isoprene photooxidation: new insights into the production of acids and organic nitrates, Atmos. Chem. Phys., 9, 1479-1501, doi:10.5194/acp-9-1479-2009, 2009.

St. Clair, J. M., Rivera-Rios, J. C., Crounse, J. D., Knap, H. C., Bates, K. H., Teng, A. P., Jørgensen, S., Kjaergaard, H. G., Keutsch, F. N., and Wennberg, P. O.: Kinetics and Products of the Reaction of the First-Generation Isoprene Hydroxy Hydroperoxide (ISOPOOH) with OH, J. Phys. Chem. A, doi: 10.1021/acs.jpca.5b06532, 2015. doi:10.1021/acs.jpca.5b06532, 2015.

Surratt, J. D., Chan, A. W. H., Eddingsaas, N. C., Chan, M., Loza, C. L., Kwan, A. J., Hersey, S. P., Flagan, R. C., Wennberg, P. O., and Seinfeld, J. H.: Reactive intermediates revealed in secondary organic aerosol formation from isoprene, Proc. Nat. Acad. Sci., 107, 6640-6645, doi:10.1073/pnas.0911114107, 2010.

Zhang, X., Cappa, C. D., Jathar, S. H., McVay, R. C., Ensberg, J. J., Kleeman, M. J., and Seinfeld, J. H.: Influence of vapor wall loss in laboratory chambers on yields of secondary organic aerosol, Proc. Nat. Acad. Sci., 111, 5802-5807, doi:10.1073/pnas.1404727111, 2014.

Sect. S2: Comparison of the default [*Jo et al.*, 2013] and the updated VBS for toluene and α-pinene oxidation.

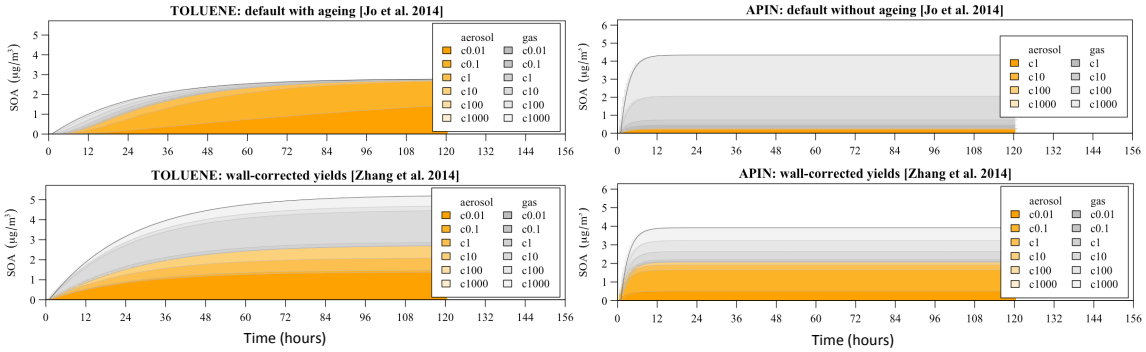

Figure S2: Distribution of the organic mass in particle (orange) and vapor (gray) phases generated from the oxidation of 1 ppbv of toluene (left) and α-pinene (right). Calculations are performed with 1 µg m^{-3} of organic aerosol seed that is used for gas-particle partitioning.

Sect. S3: Historic and wall-corrected SOA yields

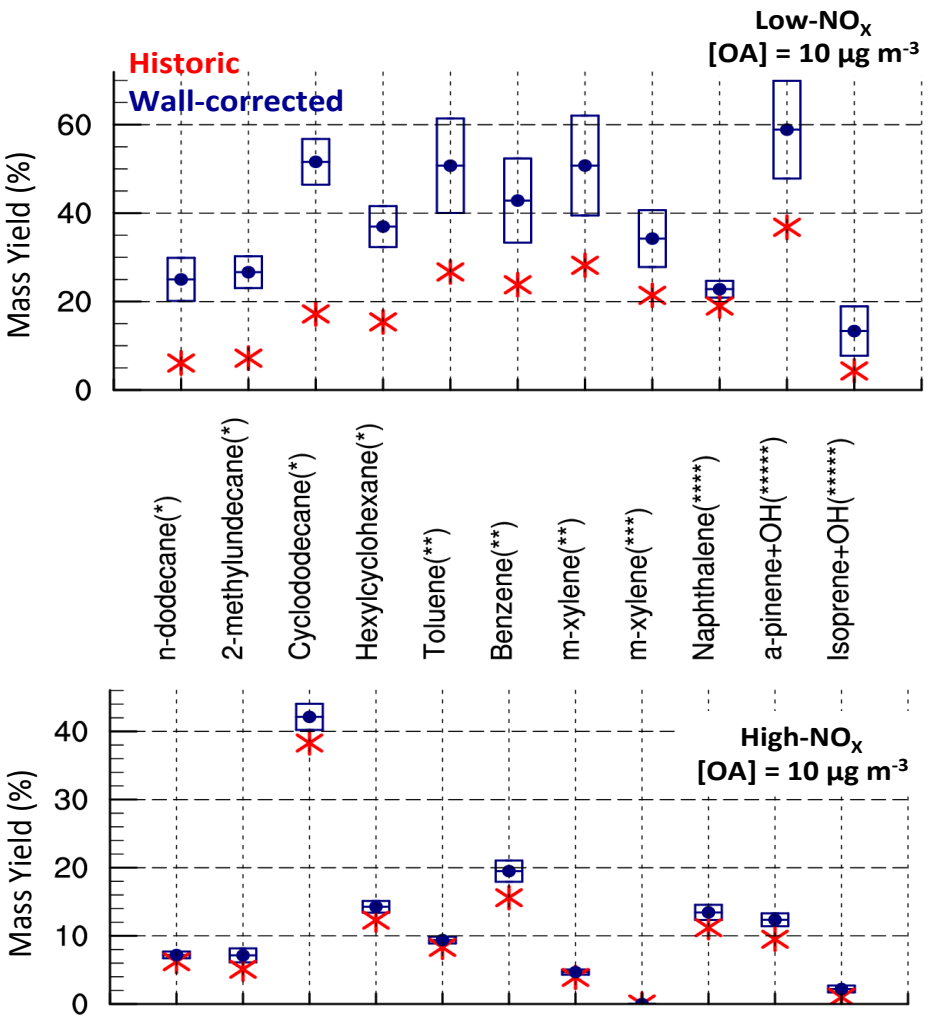

(*)Values based on the Statistical Oxidation Model (SOM) estimates [*Cappa et al.,* 2013]; (**)Yields based on *Ng et al.* [2007]; (***)Yields from *Loza et al.* [2012]; (****)Yields from *Chan et al.* [2009]; (*****)Yields based on *Chhabra et al.* [2011].

Figure S3: Comparison of historic (red) and wall corrected SOA yields (blue) reported by *Zhang et al.* [2014, Table 1] under low- and high-NO_X conditions. The average biases in SOA yields due to vapor wall losses for various VOCs are also given around the mean value (blue boxes).

Cappa, C.D., et al., Application of the Statistical Oxidation Model (SOM) to sec- ondary organic aerosol formation from photooxidation of C12 alkanes. Atmos. Chem. Phys. 13:1591–1606, 2013.

Chan AWH, et al., Secondary organic aerosol formation from photooxidation of naphthalene and alkylnaphthalenes: Implications for oxidation of intermediate volatility organic compounds (IVOCs) Atmos. Chem. Phys. 9(9):3049–3060, 2009.

Chhabra PS, et al., Elemental composition and oxidation of chamber organic aerosol. Atmos. Chem. Phys. 11(17):8827–8845, 2011.

Loza CL, et al., Chemical aging of m-xylene secondary organic aerosol: Laboratory chamber study. Atmos. Chem. Phys. 12(1):151–167, 2012.

Ng NL, et al., Secondary organic aerosol formation from m-xylene, toluene, and benzene. Atmos Chem Phys 7(14):3909–3922, 2007.

Sect. S4: Contribution of various sources to SOA production in the lower troposphere.

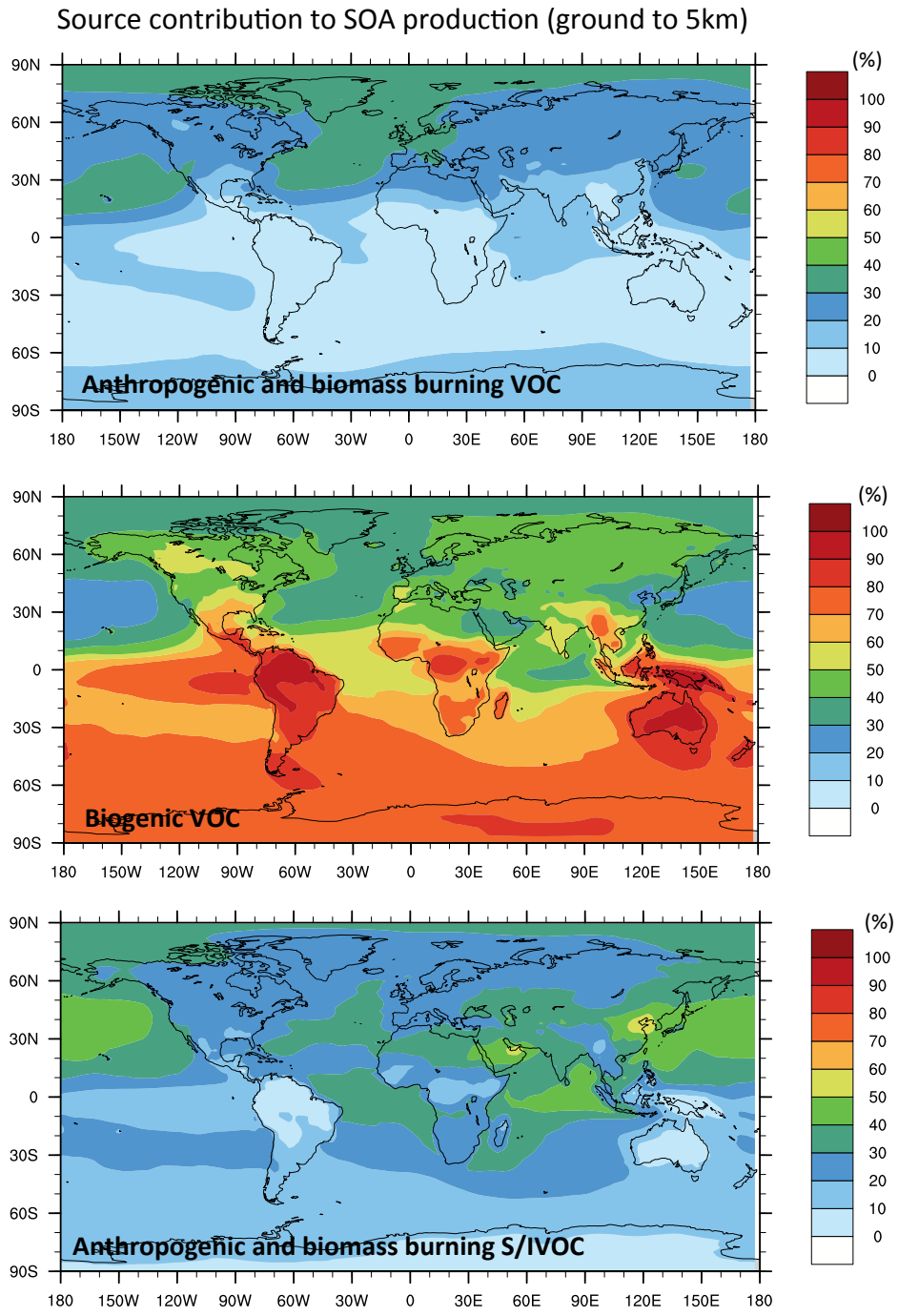

Figure S4: Relative contribution (%) of various sources to predicted SOA concentrations in the lower troposphere (ground to 5km) in the NY_DPH simulation (with the updated treatment of SOA production and removal).

Sect. S5: Description of EMEP stations and aircraft campaigns

Table S4: Sampling sites of the EMEP OC campaign in Europe used in this study. All sites are representative of the urban background locations.

Site	Country	Latitude (°N)	Longitude (°E)	Height (m, asl)
Illmitz	Austria	47.77	16.77	117
Univ. of Gent	Belgium	51.05	3.72	0
Kosetice	Czech Rep.	49.58	15.08	534
Waldhof	Germany	52.80	10.76	74
Virolahti	Finland	60.53	27.69	4
Edingburgh	Scotland	55.95	3.22	0
Mace Head	Ireland	53.17	9.5	15
Belogna	Italy	44.48	11.33	0
Kollumerwaard	Netherlands	53.33	6.28	1
Braganca	Portugal	41.82	6.77	690
Aspvreten	Sweeden	58.80	17.38	20

Table S5: Aircraft measurements of organic aerosols used in this study. Data and their detailed description can be found at https://sites.google.com/site/amsglobaldatabase/ and in *Heald et al.* [2011]. SEAC4RS data are accessible at http://www-air.larc.nasa.gov.

Campaign	Location	Period	Region
ITOP	Azores (mid-latitudes)	12 Jul. - 3 Aug. 2004	Remote
IMPEX	N. America / E. Pacific (mid-latitudes)	17 Apr. - 15 May 2006	Remote +aged
VOCALS-UK	Eastern S. Pacific (tropical)	27 Oct. - 13 Nov. 2008	Remote
ADRIEX	N. Italy / Adriatic (mid-latitudes)	27 Aug. – 6 Sep. 2004	Pollution
TexAQ	Texas region (mid-latitudes)	11 Sep. – 13 Oct. 2006	Pollution
EUCAARI	N. Europe (mid-latitudes)	6 - 22 May 2008	Pollution
SEAC4RS	SE. US (mid-latitudes)	6 Aug. – 23 Sep. 2013	Pollution /Fires
ARCTAS	Artic / N. Europe (high latitudes)	1-20 Apr. 2008; 18 Jun.-13 Jul. 2008	Fires